



Benzimidazole and imidazole inhibitors of histone deacetylases: Synthesis and biological activity

Jerome C. Bressi, Ron de Jong, Yiqin Wu, Andy J. Jennings, Jason W. Brown, Shawn O'Connell, Leslie W. Tari, Robert J. Skene, Phong Vu, Marc Navre, Xiaodong Cao, Anthony R. Gangloff*

Takeda San Diego, 10410 Science Center Drive, San Diego, CA 92121, USA

ARTICLE INFO

Article history:

Received 29 January 2010

Revised 25 March 2010

Accepted 26 March 2010

Available online 30 March 2010

Keywords:

Histone deacetylase inhibitors

HDAC

Oncology

ABSTRACT

A series of *N*-hydroxy-3-[3-(1-substituted-1*H*-benzimidazol-2-yl)-phenyl]-acrylamides (**5a–5ab**) and *N*-hydroxy-3-[3-(1,4,5-trisubstituted-1*H*-imidazol-2-yl)-phenyl]-acrylamides (**12a–s**) were designed, synthesized, and found to be nanomolar inhibitors of human histone deacetylases. Multiple compounds bearing an *N*1-piperidine demonstrate EC₅₀s of 20–100 nM in human A549, HL60, and PC3 cells, in vitro and in vivo hyperacetylation of histones H3 and H4, and induction of p21^{waf}. Compound **5x** displays efficacy in human tumor xenograft models.

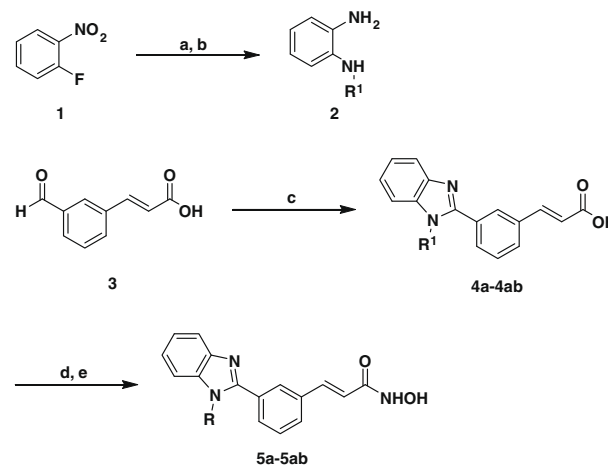
© 2010 Elsevier Ltd. All rights reserved.

The reversible acetylation of ϵ -*N*-acetyl groups of lysine residues, in the *N*-terminal tails of core histones, plays a critical role in the regulation of gene expression by altering the accessibility of transcriptional factors to DNA via conformational changes in the structure of the nucleosome.^{1–3} This restructuring of chromatin is regulated by the balance of histone acetyl transferase (HAT) and histone deacetylase (HDAC) activity.^{4,5} Perturbations of this balance have been linked to cancer, and inhibition of HDACs results in the expression of genes that produce growth arrest, terminal differentiation, and/or apoptosis in a variety of cancer cells.⁶ Inhibition of HDACs has been indicated as a unique mechanism for cancer chemotherapy, and a number of small-molecule inhibitors have advanced into clinical trials.^{7–9}

The structure of the HDAC active site is comprised of a narrow, hydrophobic tunnel originating at the protein–solvent interface and leading 8 Å into a cavity that contains the catalytic Zn²⁺. A typical HDAC inhibitor consists of a bidentate chelators tethered to a binding moiety that interacts with the mouth of the tunnel at the protein–solvent interface.¹⁰ Utilizing crystal structures of HDAC-2 and HDAC-8,¹¹ as well as capitalizing on published SAR, we designed and synthesized a variety of compounds building off of an *N*-hydroxycinnamamide. Structure-guided designs suggested that substituted five-membered rings projecting from the 3-position of *N*-hydroxycinnamamide would best facilitate productive interaction between a binding moiety and the protein surface. Our efforts to

identify novel HDAC inhibitors focused on *N*1-substituted benzimidazoles and imidazoles as binding moiety chemotypes.

The synthesis of *N*-hydroxy-3-[3-(1-substituted-1*H*-benzimidazol-2-yl)-phenyl]-acrylamides¹² (**5a–ab**, Scheme 1) begins with nucleophilic aromatic substitution of 1-fluoro-2-nitro-benzene (**1**) with the appropriate primary amine followed by reduction of the nitro group under standard conditions to provide *N*-substituted-benzene-1,2-diamines (**2**). Condensation of the aniline (**2**) with



Scheme 1. Reagents and conditions: (a) R¹NH₂, Et₃N, DMF, 60 °C, 3–48 h; (b) powdered Zn, AcOH, EtOH, reflux; (c) 2, AcOH, EtOH, reflux, 24–48 h; (d) NH₂OTHP, EDCl, HOBT, DIEA, DMF, rt, 18 h; (e) CSA, MeOH, rt, 1 h.

* Corresponding author. Tel.: +1 858 731 3531; fax: +1 858 550 0526.

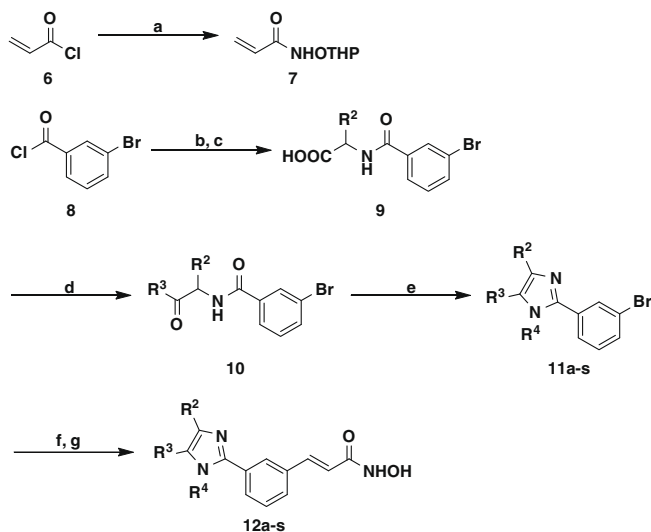
E-mail addresses: agangloff@takedasd.com, anthony.gangloff@takedasd.com (A.R. Gangloff).

3-(3-formyl-phenyl)-acrylic acid¹³ (**3**) and subsequent in situ cyclization and oxidation provides 3-[3-(1-substituted-1*H*-benzimidazol-2-yl)-phenyl]-acrylic acids (**4a–ab**). Treatment of **4a–ab** with *O*-(tetrahydropyran-2-yl)-hydroxylamine in the presence of EDCI and HOBt followed by treatment with camphorsulfonic acid yields the desired *N*-hydroxy-3-[3-(1-substituted-1*H*-benzimidazol-2-yl)-phenyl]-acrylamides (**5a–ab**).

The synthesis of *N*-hydroxy-3-[3-(1,4,5-trisubstituted-1*H*-imidazol-2-yl)-phenyl]-acrylamides¹⁴ (**12a–s**, Scheme 2) begins with acylation of the appropriate amino acid ester with 3-bromo-benzoyl chloride followed by saponification to provide the desired carboxylic acids (**9**). R³ is installed by treatment of **9** with the appropriate anhydride to provide the Dakin–West intermediate (**10**). Imine formation with the R⁴ bearing primary amine and **10** followed by in situ cyclization via microwave irradiation provides the desired 2-(3-bromo-phenyl)-1,4,5-trisubstituted-1*H*-imidazole (**11a–s**). Standard Heck coupling conditions of **11a–s** with *N*-(tetrahydro-pyran-2-yloxy)-acrylamide (**7**) and CSA mediated tetrahydropyran (THP) cleavage yields the desired *N*-hydroxy-3-[3-(1,4,5-trisubstituted-1*H*-imidazol-2-yl)-phenyl]-acrylamides (**12a–s**). Substituting the appropriate reagents, *N*-hydroxy-3-[3-(2,3,5-trisubstituted-3*H*-imidazol-4-yl)-phenyl]-acrylamides¹⁴ (**17a–f**) may be synthesized utilizing this same methodology as depicted in Scheme 3.

All compounds were screened against purified recombinant human HDAC-2, -6, and -8 enzymes and IC₅₀s were determined using known concentrations of enzyme with *t*BOC(Ac)-Lys-AMC as a substrate¹⁵ (Tables 1–3). Compounds were also evaluated in human A549 lung, HL60 leukemia, and PC3 prostate cancer cell lines (Tables 1 and 2). EC₅₀ determinations were calculated from remaining NADH levels after a 72 h compound incubation and a MTS colorimetric readout.

Chemistry efforts started with a small focused library of benzimidazoles, **5a–5t** (Table 1). With few exceptions, the enzyme activity for distinct isozymes was 10–100 nM and selectivity across isozymes was less than eightfold. The SAR could not be rationalized given that the binding moiety interacts predominantly with the protein–solvent interface. Cell viability for **5a–5t** was relatively flat with the exception of **5t**, which demonstrated low-micromolar EC₅₀s across all cell lines. Synthetic resolution of the enantiomers, **5u** and **5v**, realized a 2–6-fold potency increase for the *R*-isomer.



Scheme 2. Reagents and conditions: (a) NH₂OTHP, Et₃N, DMF, 0 °C, 18 h; (b) NH₂R²CH₂COOCH₃, Et₃N, DCM, rt, 2 h; (c) LiOH, MeOH, rt, 2 h; (d) [R³C(O)]₂O, DMAP, Et₃N, 60 °C, 30 min then HOAc, 60 °C 30 min; (e) R⁴NH₂, HOAc with microwave irradiation at 200 °C for 2 h; (f) **7**, Et₃N, Pd(OAc)₂, P(*o*-Tol)₃, DMF, 110 °C, 1 h; (g) CSA, MeOH, rt, 1 h.

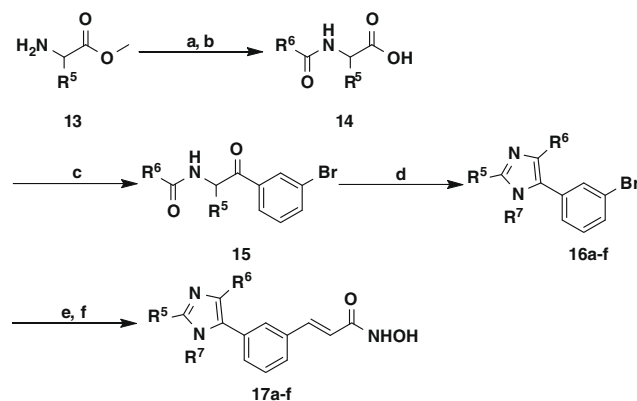
N-Methyl and *N*-ethyl piperidine derivatives, **5w–5ab**, gave similar results. The cell potency that the piperidine moiety conveyed to the benzimidazole was also realized with *N*-hydroxy-3-[3-(1,4,5-trisubstituted-1*H*-imidazol-2-yl)-phenyl]-acrylamides (Table 2). *N*-Hydroxy-3-[3-(2,3,5-trisubstituted-3*H*-imidazol-4-yl)-phenyl]-acrylamides experienced diminished binding activity compared with their structural isomers (Table 3). PK and toxicity screens showed benzimidazoles **5** as the most promising for further development compared to imidazoles **12** (data not shown).

To verify the mode of action of the benzimidazole and imidazole analogues, compounds showing potent activity in the HL60 cell viability assay were evaluated for their ability to induce hyperacetylation of histones H3 and H4 in HL60 leukemia cells. At cell effective concentrations, inhibitor treatment led to induction of histone H3 and H4 acetylation. With increasing dilution of inhibitor dropping below the effective concentration, histone acetylation returned to background levels similar to DMSO-treated control. In general, the EC₅₀s in the cellular histone acetylation in HL60 cells correlated well with HL60 cell viability EC₅₀s. This is exemplified by compounds **5x** (H3 EC₅₀ = 0.10 μM, H4 EC₅₀ = 0.11 μM) and **5aa** (H3 EC₅₀ = 0.13 μM, H4 EC₅₀ = 0.10 μM) in Figure 1.

A hallmark of HDAC inhibition is the induction of p21^{waf}, which is suspected to mediate the antiproliferative effects observed with intracellular HDAC inhibition. Compounds **5x** and **5aa** were evaluated for their ability to activate the p21^{waf} promoter using an engineered cell line containing a stably integrated luciferase reporter gene under control of the human p21 promoter. Compounds **5x** and **5aa** induced p21^{waf} activity at EC₅₀s of 0.10 μM and 0.078 μM, respectively. This is the effective concentration of compound that results in 50% of the maximum p21^{waf} induction compared with standard HDAC inhibitor trichostatin-A.

Compound **5x** was further evaluated in a xenograft pharmacodynamic assay. PANC-1 tumor bearing mice received a single intraperitoneal dose of 50 mg/kg of **5x**. Relative to vehicle control, treatment with **5x** resulted in a substantial increase in the acetylation of histones H3 and H4 in the tumor tissue (Fig. 2). Histone acetylation started to subside after 8 h and returned to background levels around 24 h. Similar results were obtained with **5aa** (data not shown).

Compound **5x** was also evaluated in a human HCT116 colon xenograft mouse model and exhibited evidence of tumor growth inhibition at the highest dose of 40 mg/kg (Table 4). Compound **5x** demonstrated a maximum T/C of 45% with mild, temporary weight losses observed in the cohorts of animals. In the PC3 prostate model using similar conditions, compound **5x** exhibited similar tumor growth inhibition (data not shown).



Scheme 3. Reagents and conditions: (a) R⁶C(O)Cl, Et₃N, DCM, rt, 2 h; (b) LiOH, MeOH, rt, 2 h; (c) [3-BrPhC(O)]₂O, DMAP, Et₃N, 60 °C, 30 min then HOAc, 60 °C, 30 min; (d) R⁷NH₂, HOAc with microwave irradiation at 200 °C for 2 h; (e) **7**, Et₃N, Pd(OAc)₂, P(*o*-Tol)₃, DMF, 110 °C, 1 h; (f) CSA, MeOH, rt, 1 h.

Table 1
HDAC enzyme inhibition and cell viability data for *N*-hydroxy-3-[3-(1-substituted-1*H*-benzimidazol-2-yl)-phenyl]-acrylamide analogues

Compd	R ¹	HDAC-2 IC ₅₀ ^a (nM)	HDAC-6 IC ₅₀ ^a (nM)	HDAC-8 IC ₅₀ ^a (nM)	A549 EC ₅₀ ^b (μM)	HL60 EC ₅₀ ^b (μM)	PC3 EC ₅₀ ^b (μM)
5a	H	100	100	63.0	25	3.1	10
5b	Me	120	79.0	100	12	2.0	7.9
5c	<i>i</i> -Pr	79.0	100	40.0	5.0	1.0	2.5
5d	Cyclohexyl	25.0	25.0	50.0	3.1	0.5	1.6
5e	–CH ₂ CH ₂ N(Me) ₂	63.0	79.0	160	7.9	1.0	2.5
5f	–CH ₂ CH ₂ N(Et) ₂	31.0	79.0	63.0	4.0	0.8	1.2
5g	–CH ₂ CH ₂ N(<i>i</i> -Pr) ₂	40.0	100	200	5.0	5.0	3.1
5h	–CH ₂ CH ₂ - <i>N</i> -morpholine	50.0	160	400	25	1.2	5.0
5i	–CH ₂ -4-piperidine	160	200	310	>50	>50	>50
5j	–CH ₂ CH ₂ - <i>N</i> -piperidine	10.0	40.0	100	1.2	0.3	0.6
5k	–CH ₂ CH ₂ - <i>N</i> -pyrrolidine	16.0	63.0	63.0	3.1	0.5	0.6
5l	Ph	63.0	50.0	50.0	16.0	1.6	4.0
5m	4-Cl-Ph	50.0	100	50.0	6.3	0.8	2.5
5n	4-OMe-Ph	40.0	63.0	63.0	4.0	0.5	1.2
5o	–CH ₂ CH ₂ Ph	7.90	31.0	25.0	2.5	0.3	0.4
5p	–CH ₂ CH ₂ CH ₂ Ph	12.0	20.0	25.0	12	1.2	4.0
5q	Bn	50.0	63.0	40.0	6.3	5.0	1.2
5r	(<i>R</i>)-α-Me-Bn	25.0	40.0	20.0	16	3.1	10
5s	(<i>S</i>)-α-Me-Bn	63.0	63.0	16.0	31	3.1	16
5t	–(±)-3-piperidine	20.0	40.0	160	2.5	0.3	0.5
5u	–(<i>R</i>)-3-piperidine	12.0	79.0	120	1.0	0.1	0.1
5v	–(<i>S</i>)-3-piperidine	12.0	25.0	120	2.5	0.3	0.6
5w	–(±)- <i>N</i> -Me-3-piperidine	25.0	79.0	160	0.5	0.08	0.1
5x	–(<i>R</i>)- <i>N</i> -Me-3-piperidine	10.0	100	200	0.3	0.04	0.05
5y	–(<i>S</i>)- <i>N</i> -Me-3-piperidine	16.0	50.0	160	1.2	0.16	0.3
5z	–(±)- <i>N</i> -Et-3-piperidine	20.0	79.0	120	0.5	0.06	0.1
5aa	–(<i>R</i>)- <i>N</i> -Et-3-piperidine	10.0	79.0	120	0.2	0.03	0.05
5ab	–(<i>S</i>)- <i>N</i> -Et-3-piperidine	31.0	79.0	160	0.6	0.08	0.2

^a IC₅₀ values are the mean of at least three experiments, and statistical error limits have been calculated and amount to 10% or less.

^b EC₅₀ values are the mean of at least two experiments, and statistical error limits have been calculated and amount to 25% or less.

Table 2
HDAC enzyme inhibition and cell viability data for *N*-hydroxy-3-[3-(1,4,5-trisubstituted-1*H*-imidazol-2-yl)-phenyl]-acrylamide analogues.

Compd	R ²	R ³	R ⁴	HDAC-2 IC ₅₀ ^a (nM)	HDAC-6 IC ₅₀ ^a (nM)	HDAC-8 IC ₅₀ ^a (nM)	A549 EC ₅₀ ^b (μM)	HL60 EC ₅₀ ^b (μM)	PC3 EC ₅₀ ^b (μM)
12a	Ph	Me	–CH ₂ CH ₂ - <i>N</i> -morpholine	10.0	63.0	79.0	6.3	0.3	1.0
12b	Ph	Me	–CH ₂ CH ₂ Ph	5.00	63.0	20.0	0.8	0.2	0.3
12c	Ph	Me	–(<i>R</i>)- <i>N</i> -Me-3-piperidine	5.00	63.0	50.0	0.6	0.04	0.1
12d	Ph	Me	–(<i>R</i>)- <i>N</i> -Et-3-piperidine	6.30	100	31.0	0.3	0.03	0.05
12e	Ph	Me	–(<i>R</i>)- <i>N</i> - <i>i</i> -Pr-3-piperidine	5.00	79.0	31.0	0.5	0.04	0.1
12f	Me	Ph	–CH ₂ CH ₂ - <i>N</i> -morpholine	31.0	120	79.0	4.0	0.3	1.0
12g	Me	Ph	–CH ₂ CH ₂ Ph	7.90	79.0	25.0	1.0	0.3	0.5
12h	Me	Ph	–(<i>R</i>)- <i>N</i> -Me-3-piperidine	10.0	79.0	100	0.4	0.03	0.1
12i	Me	Ph	–(<i>R</i>)- <i>N</i> -Et-3-piperidine	7.90	79.0	50.0	0.3	0.04	0.08
12j	Me	Ph	–(<i>R</i>)- <i>N</i> - <i>i</i> -Pr-3-piperidine	6.30	100	40.0	0.4	0.03	0.2
12k	Bn	Me	–CH ₂ CH ₂ - <i>N</i> -morpholine	12.0	79.0	50.0	4.0	0.3	1.0
12l	Bn	Me	–CH ₂ CH ₂ Ph	7.90	63.0	16.0	0.8	0.2	0.5
12m	Bn	Me	–(<i>R</i>)- <i>N</i> -Me-3-piperidine	6.30	63.0	79.0	0.2	0.02	0.1
12n	Bn	Me	–(<i>R</i>)- <i>N</i> -Et-3-piperidine	10.0	100	50.0	0.1	0.03	0.04
12o	Me	Bn	–CH ₂ CH ₂ - <i>N</i> -morpholine	10.0	79.0	63.0	2.5	0.2	0.6
12p	Me	Bn	–CH ₂ CH ₂ Ph	5.00	50.0	20.0	0.3	0.05	0.2
12q	Me	Me	–CH ₂ CH ₂ - <i>N</i> -morpholine	31.0	160	200	>50	1.6	5.0
12r	Me	Me	–CH ₂ CH ₂ Ph	7.90	63.0	31.0	0.4	0.08	0.2
12s	Me	Me	–(<i>R</i>)- <i>N</i> -Et-3-piperidine	12.0	120	100	0.3	0.04	0.08

^a IC₅₀ values are the mean of at least three experiments, and statistical error limits have been calculated and amount to 10% or less.

^b EC₅₀ values are the mean of at least two experiments, and statistical error limits have been calculated and amount to 25% or less.

Table 3
HDAC enzyme inhibition data for *N*-hydroxy-3-[3-(2,3,5-trisubstituted-3*H*-imidazol-4-yl)-phenyl]-acrylamide analogues

Compd	R ⁵	R ⁶	R ⁷	HDAC-2 IC ₅₀ ^a (nM)	HDAC-6 IC ₅₀ ^a (nM)	HDAC-8 IC ₅₀ ^a (nM)
17a	Me	Me	–CH ₂ CH ₂ Ph	79	120	100
17b	Me	Me	–(<i>R</i>)- <i>N</i> -Et-3-piperidine	500	400	500
17c	Ph	Me	–CH ₂ CH ₂ Ph	79	79	50
17d	Ph	Me	–(<i>R</i>)- <i>N</i> -Et-3-piperidine	630	630	400
17e	Bn	Me	–CH ₂ CH ₂ Ph	40	63	63
17f	Bn	Me	–(<i>R</i>)- <i>N</i> -Et-3-piperidine	120	500	100

^a IC₅₀ values are the mean of at least three experiments, and statistical error limits have been calculated and amount to 10% or less.

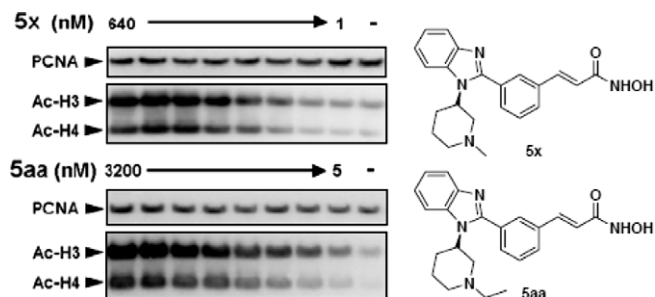


Figure 1. Induction of histone H3 and H4 acetylation by compounds **5x** and **5aa** in HL60 leukemia cells. Cells were treated for 4 h with 2.5-fold serial dilutions of compound. Control DMSO-treated cells are indicated with hyphen. Histone acetylation in whole cell lysates was analyzed by Western blotting. PCNA antibodies were used as a control for protein loading. Dose–response signals were quantified in order to calculate the inhibitor concentration giving the half-maximal response.

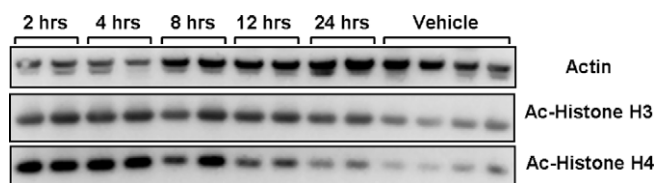


Figure 2. Increased acetylation of histones in PANC-1 xenograft in nude mice after administration of 50 mg/kg **5x**. At indicated time points, tumors were harvested and whole tissue lysates were prepared and analyzed by Western blotting. Histone acetylation was detected by antibodies specific for acetylated Histone H3 or H4, respectively. Actin antibodies were used as a control for protein loading.

In conclusion, a series of benzimidazole and imidazole cinnamoyl hydroxamates were shown to inhibit recombinant human HDACs in the low nanomolar range. Incorporation of an N1-piperidine into both benzimidazole and imidazole scaffolds conveyed cellular potency and resulted in analogues demonstrating killing of human cancer cells in the sub-micromolar range. Compounds **5x** and **5aa** induced acetylation of histones H3 and H4 in vitro and in vivo as well as induced p21^{waf} activity. Compound **5x** also exhibited moderate tumor growth inhibition in a HCT116 xeno-

Table 4

In vivo antitumor activity of compound **5x** against human HCT116 colon carcinoma xenograft^a

Compd	Dose ^b (mg/kg)	%T/C ^c (%)	Δ% Body weight ^d (day 6)
5x	15	66	+1.7
5x	25	47	–2.5
5x	40	45	–3.6

^a Each treatment group contained 10 mice.

^b Compounds were administered intraperitoneally, qdx5 per week, in total 15 doses.

^c %T/C values were calculated when vehicle-treated mice reached 1 g median size, which was 10 days after the last dose.

^d Maximum body weight loss at the nadir.

graft mouse model. Overall, the compounds described add to the body of knowledge of HDAC inhibitors with novel substituents at the protein–solvent interface which confer not only enzymatic activity but also cellular and in vivo activity.

References and notes

- Kouzarides, T. *Curr. Opin. Genet. Dev.* **1999**, *9*, 40.
- Strahl, B. D.; Allis, C. D. *Nature* **2000**, *403*, 41.
- Lane, A. A.; Chabner, B. A. *J. Clin. Oncol.* **2009**, *27*, 5459.
- Eberharter, A.; Becker, P. B. *EMBO Rep.* **2002**, *3*, 224.
- Grozinger, C. M.; Schreiber, S. L. *Chem. Biol.* **2002**, *9*, 6.
- Bolden, J. E.; Peart, M. J.; Johnstone, R. W. *Nat. Rev. Drug Disc.* **2006**, *5*, 769.
- Kristeleit, R.; Fong, P.; Aherne, G. W.; de Bono, J. *Clin. Lung Cancer* **2005**, *S19*.
- Botrugno, O. A.; Santoro, F.; Minucci, S. *Cancer Lett.* **2009**, *280*, 184.
- Ma, X.; Ezzeldin, H. H.; Diasio, R. B. *Drugs* **2009**, *69*, 1911.
- (a) Giannini, G.; Marzi, M.; Pezzi, R.; Brunetti, T.; Battistuzzi, G.; Di Marzo, M.; Cabri, W.; Vesci, L.; Pisano, C. *Bioorg. Med. Chem. Lett.* **2009**, *19*, 3694; (b) Su, H.; Yu, L.; Nebbioso, A.; Carafa, V.; Chen, Y.; Altucci, L.; You, Q. *Bioorg. Med. Chem. Lett.* **2009**, *19*, 6284.
- Somoza, J. R.; Skene, R. J.; Katz, B. A.; Mol, C.; Ho, J. D.; Jennings, A. J.; Luong, C.; Arvai, A.; Buggy, J. J.; Chi, E.; Tang, J.; Sang, B.-C.; Verner, E.; Wynands, R.; Leahy, E. M.; Dougan, D. R.; Snell, G.; Navre, M.; Knuth, M. W.; Swanson, R. V.; Mcrea, D. E.; Tari, L. W. *Structure* **2004**, *12*, 1325.
- Synthetic details and characterization data can be found in: Bressi, J. C.; Brown, J. W.; Cao, S. X.; Gangloff, A. R.; Jennings, A. J.; Stafford, J. A.; Vu, P. H.; Xiao, X.-Y. U.S. Patent 7169,801, **2007**.
- Kumar, S.; Kapoor, K. K. *Synlett* **2007**, *18*, 2809.
- Synthetic details and characterization data can be found in: Bressi, J. C.; Cao, S. X.; Gangloff, A. R.; Jennings, A. J.; Stafford, J. A. U.S. Patent Appl. 2005/0159470, **2005**.
- Wegener, D.; Hildmann, C.; Riester, D.; Schober, A.; Meyer-Almes, F.-J.; Deubzer, H. E.; Oehme, I.; Witt, O.; Lang, S.; Jaensch, M.; Makarov, V.; Lange, C.; Busse, B.; Schwienhorst, A. *Biochem. J.* **2008**, *413*, 143.